Journal of Alloys and Compounds 509 (2011) 8337–8344

Contents lists available at ScienceDirect

Journal of Alloys and Compounds

journal homepage: www.elsevier.com/locate/jallcom

Review

Influence of austenitic orientation on martensitic transformations in a compressed high manganese steel

T.-Y. Liu, P. Yang*, L. Meng, F.-Y. Lu

School of Materials Science and Engineering, Xue Yuan Rd. 30, 100083, Beijing, China

ARTICLE INFO

Article history:
Received 7 June 2010
Received in revised form 3 May 2011
Accepted 4 May 2011
Available online 12 June 2011

Keywords:
High manganese steel
Compression
Martensitic transformation
EBSD
Orientation relationship

ABSTRACT

High manganese TRIP/TWIP steels contain two types of martensite and the morphology, size, variant selection and texture of both types of martensite are influenced by the parent austenite grain orientation. In the present paper the TRIP effect was investigated in a compressed high manganese steel, focusing on the crystallographic behavior by means of X-ray diffraction and the electron back scatter diffraction (EBSD) technique. It is observed that γ austenite oriented with ⟨1 0 0⟩ close to the compression axis (CA) transformed more easily into α′-martensite with only one variant, whereas the transformation in CA//⟨1 1 0⟩ and ⟨1 1 1⟩-oriented austenite was sluggish and often yielded several variants. This orientation dependency was ascribed to the ease of either deformation twinning or Shockley dislocation movement. Similarly, ε-M was also observed to transform smoothly into α′-M in nearly ⟨1 0 0⟩-oriented austenite and more sluggishly in other austenite grains of other orientations. However, the number of ε-M variants detected by EBSD was higher than direct observation. In contrast to thermally induced martensitic transformations, the TRIP effect during compression failed to cause grain refinement in the transformed α′-M. The rapid formation of α′-M in ⟨1 0 0⟩-oriented γ promoted the formation of a ⟨1 0 0⟩ texture of the α′-M, whereas the ⟨1 1 0⟩ texture developed in the austenite at high level of compression led to a restricted transformation into martensite. The reasons for the occurrence of a ⟨1 0 0⟩ texture in the α′-M and for the behavior of the ε-M are discussed.

Contents

1. Introduction

There are two kinds of TRIP (transformation induced plasticity) steels, namely TRIP-H and TRIP-L steels. In general TRIP-H steels contain a high level of alloying elements and TRIP-L steels only contain a low content of alloying elements. TRIP-L steels are often referred to as TRIP-assisted steels, and generally contain less than 15% residual austenite, so that in these steels the austenite orientation can only have a weak influence on martensitic transformation during plastic deformation. It is generally accepted that there are two mechanisms responsible for the TRIP effect: strain accommodation due to variant selection as proposed by Magee [1] and the strain accommodation suggested by Greenwood and Johnson [2]. The latter states that the high strain induced by newly transformed harder martensite can be transferred into the surrounding softer austenite or ferrite. For TRIP-H steels, such as stainless steels and high manganese steels, the dominant mechanism for strain accommodation during deformation is expected to be variant selection,

* Corresponding author. Tel.: +86 10 82376968; fax: +86 10 62332336.
E-mail address: yangp@mater.ustb.edu.cn (P. Yang).

0925-8388/$ – see front matter © 2011 Elsevier B.V. All rights reserved.
doi:10.1016/j.jallcom.2011.05.015

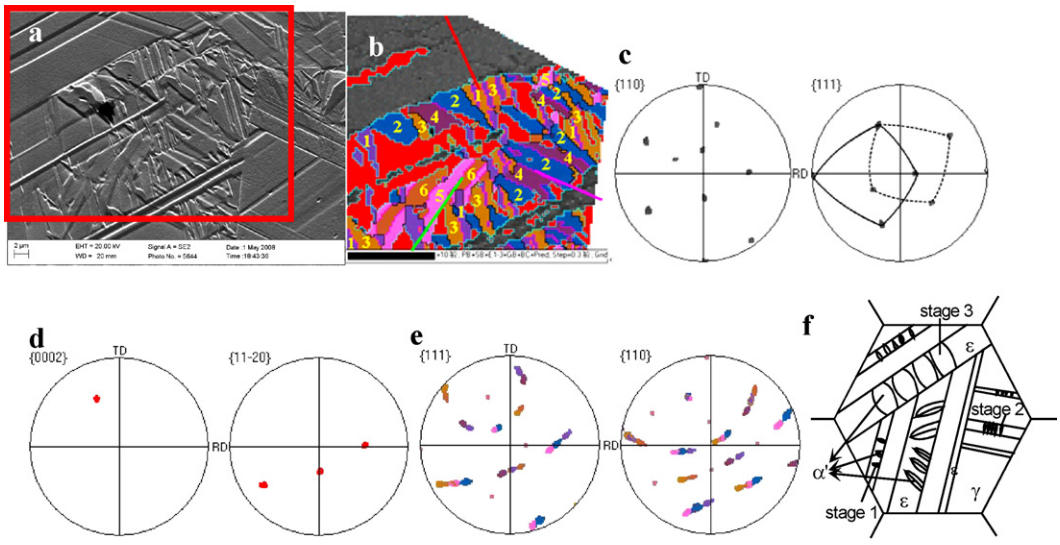

Fig. 1. EBSD-based crystallographic analysis of thermally-induced martensite in a 18Mn steel. (a) Micrograph; (b) orientation map, γ: grey; ε-M: red; α′-M: other colors according to three Euler angles; the 3 lines show the trace of interface among 3 pairs of twin-related α′-M variants. (c) Pole figures of γ; (d) pole figures of ε-M; (e) pole figures of α′-M; (f) schematic drawing showing the phase transformation and the refinement of α′-M due to restricted thickness of the ε-M. (For interpretation of the references to color in this figure legend, the reader is referred to the web version of the article.)

whereas for TRIP-L steels the dominant mechanism should be strain accommodation in the softer phase.

As a nearly fully austenitic (γ) structure can be retained at room temperature in Fe–Cr–Ni stainless steels and high manganese steels, the γ orientation and texture can significantly affect the martensitic transformation. According to the results of Kireeva and Chumlyakov [3] on single crystal stainless steels of Fe–Cr–Ni, tension-deformed at 77 K, martensite appeared asynchronously in differently oriented austenite, showing distinct plastic elongations. Their investigation revealed a close relationship between the austenitic orientation and the rate of martensitic transformation, and also demonstrated the interactions between twinning, phase transformation and shear banding associated with high elongations in TRIP steels. According to their results [3], single crystals of most easily transformed austenitic orientations, such as ⟨1 1 0⟩, did not, however, give the highest elongation during tension. Petit et al. [4] observed a slower transformation in austenitic grains with ⟨1 0 0⟩ parallel to the rolling direction and a much faster transformation in grains with ⟨1 1 1⟩ parallel to rolling direction in rolled stainless steels. Similarly, Creuziger and Foecle [5] calculated the transformation potential of martensite and demonstrated the importance of austenite orientation. From a calculation of Schmid factors, Zhang et al. [6] was able to explain experimental observations that martensite formed easily in Cube- and Goss-oriented austenite during tension, but was difficult to form in ⟨1 1 1⟩-oriented austenite during compression. Nagy et al. [7] also observed the transformation at low strains of α′-M from ⟨1 1 0⟩ austenite and noted final ⟨1 1 0⟩ texture in α′-M following tensile testing. The predictions regarding the influence of austenite orientation on the extent and speed of martensitic transformation are not always in agreement with experimental results, and moreover the presence of the intermediate ε-M phase further complicates such analyses. The orientation dependence of the martensitic transformation in polycrystalline γ in the case of the presence of two types of martensite is not so clear and requires further detailed study.

Stainless steel and high manganese steel are similar in that they both contain α′ and ε martensite. High manganese steel is considered, however, to be a better material for use in the future of structural parts of automobiles by virtue of its lower price and the fact that the TRIP effect occurs nearer to room temperature as compared to stainless steels [4,7–12]. In the present work a polycrystalline high manganese steel of composition Fe–0.15%C–18%Mn–3%Si–3%Al has been studied in order to understand the effect of austenitic orientation on martensite transformation under compression. Owing to the occurrence intermediate ε-M, it is expected that the size, orientation and even the

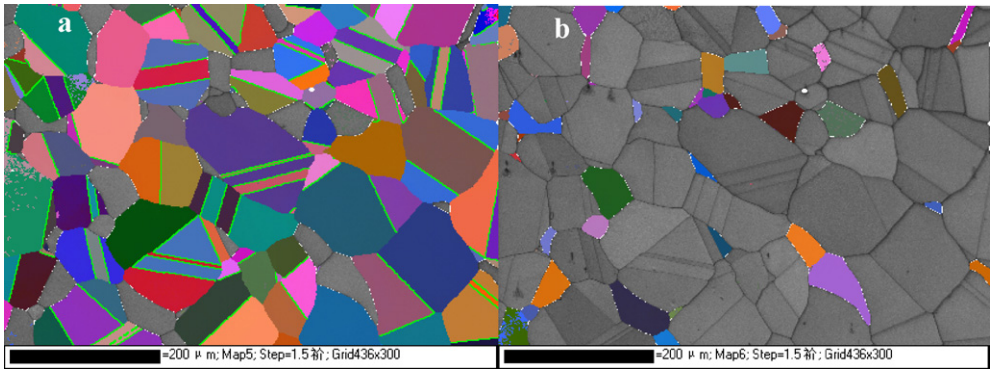

Fig. 2. Orientation maps of the sample after solution treatment followed by quenching in water. (a) Ferrite in grey and austenite colored according to the Euler angles; annealing twins are marked in green lines; (b) Kikuchi band contrast map of austenite (grey) with ferrite colored according to the three Euler angles. (For interpretation of the references to color in this figure legend, the reader is referred to the web version of the article.)

hardness of the ε-M could influence the formation of α′-M significantly, which may lead to asynchronization of the ε-M and α′-M transformations. It is also expected that mechanical twinning may influence the transformation process due to the close relationship between twinning and the formation of hexagonal ε-M. Therefore the orientation dependence of transformation in high Mn TRIP/TWIP steels is likely to be very complicated and deserves detailed characterization. The main objective of this paper is to show the orientation dependence of these transformations during compression. In addition, the effect of twinning on the martensitic transformation, the characteristics of the intermediate ε-M and the texture developed during compression are also discussed.

2. Experimental procedure

The TRIP steel used in this study contained 18.40%Mn, 0.15%C, 3.26%Si and 3.01%Al (all weight percent). Cylindrical samples of Ø10 mm × 12 mm were cut from a forged plate and then heated to 1100 °C for 1 h, followed by quenching into water, so as to suppress martensitic transformation during cooling. Samples were subjected to compression reductions of between 10% to 40% on a CMT electronic universal testing machine at room temperature at a strain rate of 0.01/s. The compressed samples were electrolytically polished at a voltage of 25 V at room temperature in a solution of 5 vol% perchloric acid and 95 vol% alcohol. Macro-texture data were determined using a Siemens D-5000 X-ray diffractometer under Mo K_α radiation. Three incomplete pole figures, {1 1 1} {1 1 3} and {2 0 0}, were measured. In this paper the texture is represented in the $\varphi_2 = 45°$ section of the calculated orientation distribution function (ODF), with ND in an orientation expression in Miller index being parallel to the compression axis. The micro-texture was analyzed using an electron backscatter diffraction (EBSD) system mounted on a Zeiss Supra 55 field-emission gun scanning electron microscope (SEM).

3. Results and analyses

In order to allow a clear comparison of the transformation behavior between thermally induced martensite and strain-induced martensite, Fig. 1 shows an orientation map of the thermally induced martensite in a similar high manganese steel, with composition of Fe–0.0045C–17.48Mn–3.04Si–1.80Al (wt.%), after quenching. This steel does not contain ferrite, but water quenching does not prevent the formation of martensite. It can be seen from Fig. 1 that the thermally induced α′-M only forms within regions of ε-M (Fig. 1b) and that K–S orientation relationship (OR) exists between the austenite and the α′-M, although this is actually a combination of the Shoji–Nishiyama OR and the Burgers OR (see Fig. 1c–e). In addition, all 6 possible α′-M variants can be found in one ε-M variant, which means that no variant selection occurs during this transformation. The transformation process of two kinds of martensite is illustrated in Fig. 1f, which also shows that the α′ M size is strongly influenced by the thickness of the ε-M plates. In this way the length of the α′-M (lenticular type) can be controlled through the control of the thickness of the ε-M plates and grain refinement of α′-M can take place in the absence of variant selection. In addition, no strong texture is seen, as expected due to the presence of a large number of variants.

Fig. 2 shows an EBSD orientation map of a quenched but undeformed sample of the steel used in this study, with a higher carbon content of 0.15%. The map illustrates the presence of equiaxed ferrite rather than lenticular α′-M. From two separate orientation maps the austenite volume fraction was determined as 88.7% and the ferrite volume fraction as 11.3%, with both of these phases were nearly random oriented. Therefore thermally induced martensite was avoided during quenching of this steel. According to [13], the formation of ferrite can enrich the remaining austenite with carbon due to carbon partitioning, and in this way austenite is stabilized against martensitic transformation during cooling to room temperature. During subsequent deformation, however, this metastable austenite can then transform into martensite.

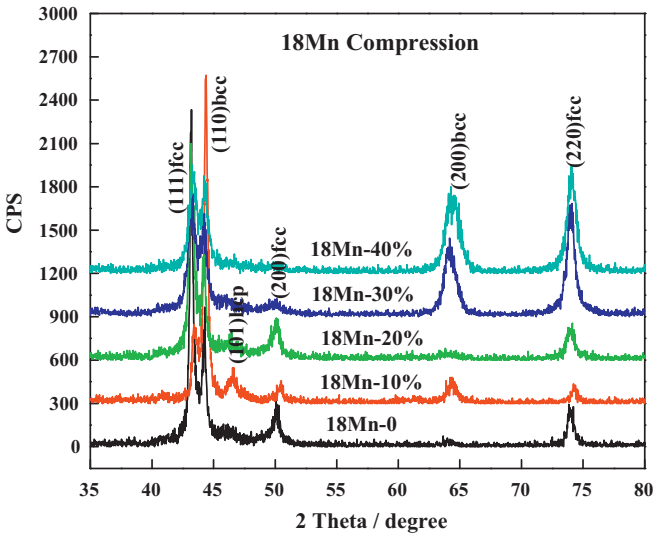

Fig. 3. XRD scan of samples compressed by different strains.

Fig. 3 shows X-ray diffraction (XRD) data for samples compressed by different reductions. The un-deformed sample illustrates the coexistence of the austenite and ferrite phases (see also Fig. 2). Therefore the analysis of α′-M by XRD will be affected by the presence of ferrite. With increasing strain, the {2 0 0}γ peak disappears, and the {1 0 1}ε peak increases slightly and then disappears, whereas the {2 2 0}γ and {2 0 0}α peaks both increase. The former indicates the texture of mechanically stabilized austenite and the latter demonstrates the texture in both ferrite and α′-M.

Fig. 4 shows examples of the microstructural evolution in samples compressed to different reductions. It is seen that martensite mainly formed only in a few selected austenitic grains, and that in these grains the angles between the martensitic variants in sample surface place are often about 90°, as shown in arrows in Fig. 4a. This observation suggests these grains may have surface normal close of ⟨1 0 0⟩ and that the martensite transformation takes place more readily in grains with this direction parallel to the compression axis. It can be noted also that according to Schmid factor calculation, this type of orientation is also prone to twinning during compression [14]. As the strain is increased to 40% (Fig. 4c), previously straight boundaries of martensite evolve into a curved configuration and the details of the martensite are difficult to identify.

Fig. 5 shows the macro-textures of the samples presented as ODF sections. A weak texture is observed in the un-deformed samples and in the 20% compressed sample (Fig. 5a, b). The texture intensity increases with further compression, evolving into a well defined ⟨1 1 0⟩ fiber texture (Fig. 5c) after a reduction of 40%, which is typical in compressed FCC metals. As compression along ⟨1 1 0⟩ does not favor deformation twinning [14], the formation of a ⟨1 1 0⟩ texture indicates that martensitic transformation was nearly complete and large misoriented areas and crystal defects yielded simultaneously, which was severely unfavorable for the shearing-type martensitic transformation. Further deformation of remaining austenite will be mainly accomplished through slip and accordingly gives rise to mechanical stabilization in austenite.

To find out dependence of the extent of transformation on austenitic grain orientation, the orientations of 101 austenitic grains which promoted martensitic transformation were measured in a 20% compressed sample. These orientations are shown in Fig. 6, which reveals that martensitic transformation takes place preferentially in austenite grains with compression directions in the region within ⟨1 0 0⟩–⟨1 1 3⟩–⟨0 1 2⟩ (i.e., around the ⟨1 0 0⟩ corner of the unit triangle). This observation is clearly in agreement with

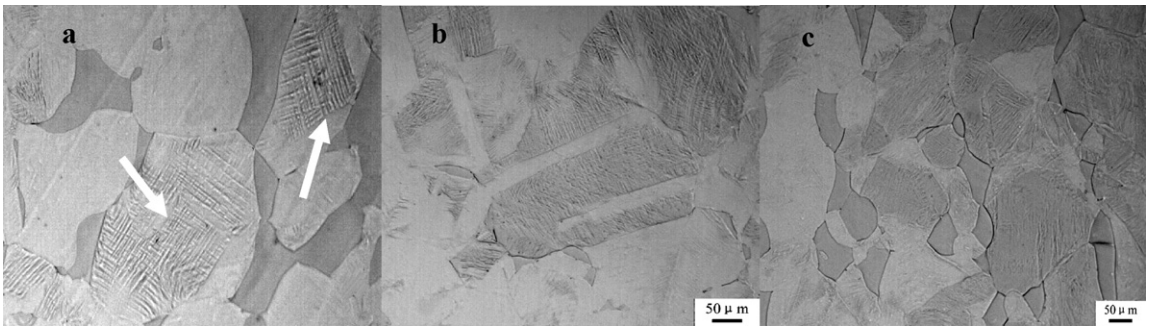

Fig. 4. Micrographs of compressed samples on compressed section. (a) 10% compression, ferrite: dark color; (b) 20% compression; (c) 40% compression.

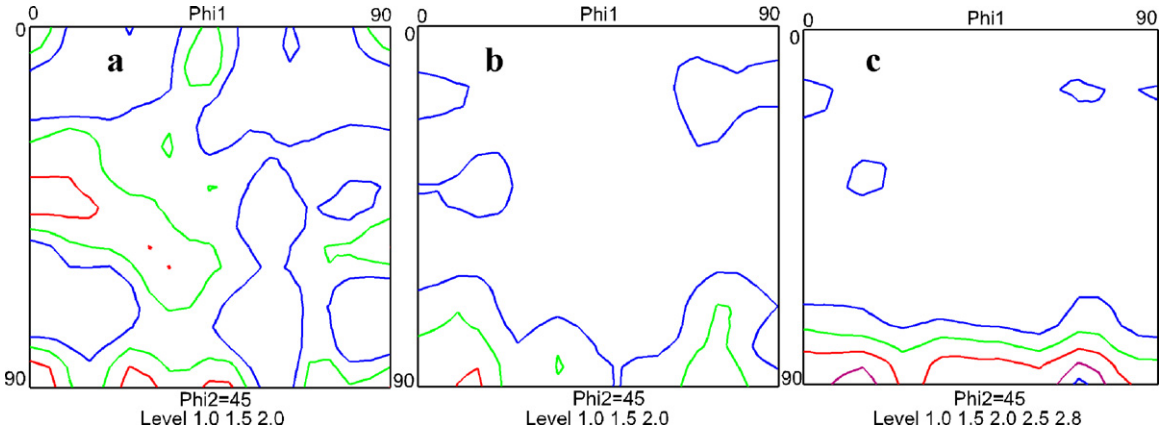

Fig. 5. Macrotexture of austenite on the cross section of compressed samples, ODF $\varphi_2 = 45^\circ$ with ND in an orientation expression in Miller index being parallel to compression axis. (a) Undeformed sample; (b) sample of compression deformed 20%; (c) sample of compression deformed 40%.

easier twinning orientation under compression. In contrast, Fig. 5c shows the orientations of grains in which no transformation took place, and it is seen that most of these grains have a compression direction close to ⟨1 1 0⟩.

To illustrate the details of the local martensitic transformations, EBSD orientation mapping was performed on 22 local regions, which cover 8 ⟨1 0 0⟩-, 2 ⟨1 1 1⟩-, 6 ⟨1 1 2⟩/⟨1 1 3⟩-, 2 ⟨1 2 4⟩- and 4 ⟨1 1 0⟩-oriented austenite grains, in samples after 10% or 20% compression. In addition to the demonstration of easy transformation in ⟨1 0 0⟩-oriented austenite and sluggish transformation in ⟨1 1 0⟩-oriented austenite, the observations also provide information about the variant selection in different austenite grains. In the following several examples are described to illustrate these points.

Fig. 7 shows an orientation map in a ⟨1 0 0⟩-oriented γ after 10% compression. Two deformation twin variants (pink and green), as well as ε-M and α′-M, are seen (Fig. 7d–f). Moreover, at least three very small ε-M variants are revealed, as shown in Fig. 7e.

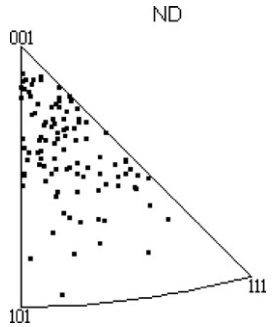

Fig. 6. Austenitic grain orientations promoting transformations in a 20% compressed sample.

These ε-M variants are more frequently distributed in the vicinity of non-indexed regions, i.e. in highly strained regions, which gives evidence of their softness and unstable orientation (hexagonal structure). Therefore most of ε-M was not severely deformed and could easily transform into α′-M. Only one large α′-M variant is seen in this grain, and no grain refinement of the α′-M was achieved, in contrast to the case of thermally induced α′-M (Fig. 1f). As one α′-M variant can only be formed in one ε-M variant, the intersected ε-M variant must accumulate a high strain in order to favor the successful α′-M variant, as only in this way can the strain be concentrated enough to induce the ($\varepsilon \rightarrow \alpha'$) transformation [10,13]. Inspection of the pole figures for the 3 phases (Fig. 7d–f), shows that the K–S OR was met in the TRIP process. This example grain shows a strong variant selection of the α′-M, and thus no effect of grain refinement during TRIP deformation, as well as the role of mechanical twinning and multiple ε-M variants.

Fig. 8 shows an orientation map for a ⟨1 1 3⟩-oriented γ grain (close to ⟨1 0 0⟩ orientation) after 10% compression. Four ε-M variants were formed (Fig. 8e), and they all lead to mostly only one ⟨1 0 0⟩-oriented α′-M, as depicted in Fig. 8f. The martensitic transformation in this grain was also affected by deformation twinning of only one variant (see Fig. 8d). The orientation of the austenite has also rotated during deformation because it is less stable than the ⟨1 0 0⟩ orientation. This grain shows an example of the rotation of the austenite orientation approximately around one of the ⟨1 1 0⟩ poles due to its unstable nature, and the feature of α′-M orientation. Otherwise the grain shows a similar behaviors to the region shown in Fig. 7.

Fig. 9 shows an orientation map of a region containing an annealing twin (see Fig. 9d) close to ⟨1 2 4⟩-oriented γ after 10% compression. No α′-M was formed in the ⟨1 1 0⟩-oriented γ (purple color in Fig. 9a, d), while several variants were formed in the

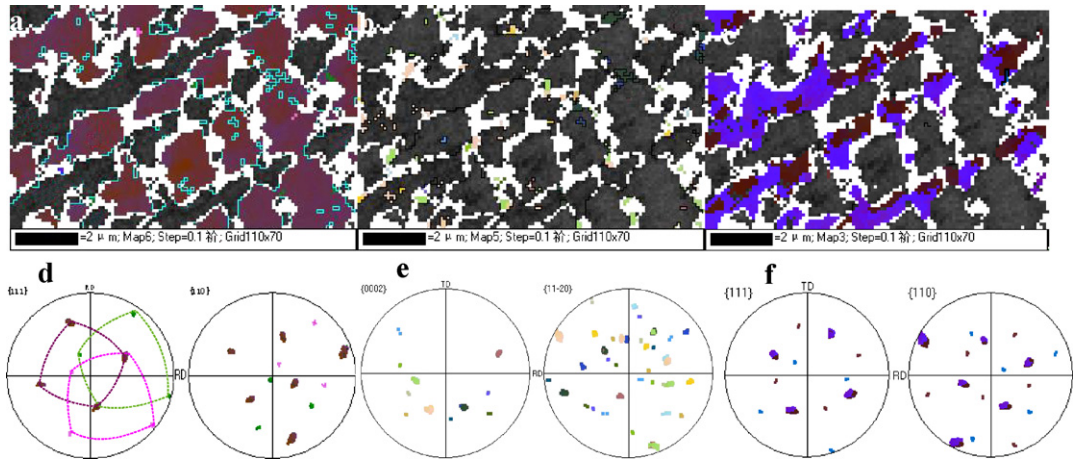

Fig. 7. Orientation maps showing martensitic transformation in ⟨1 0 0⟩-oriented γ after 10% compression. (a) Orientation map, γ: Euler angle coloring; (b) orientation map, ε-M: Euler angle coloring; (c) orientation map, α′-M: Euler angle coloring; (d) pole figures of γ showing a pair of twins; (e) pole figure of ε-M; (f) pole figure of α′-M. (For interpretation of the references to color in this figure legend, the reader is referred to the web version of the article.)

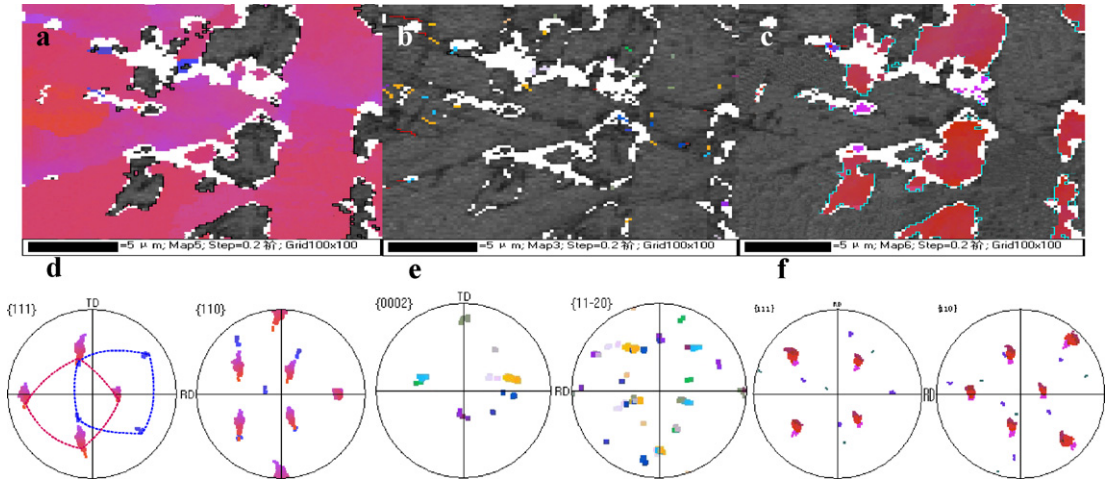

Fig. 8. Martensitic transformation in ⟨1 1 3⟩-oriented γ under 10% compression. (a) Orientation map, γ: Euler angle coloring; (b) orientation map, ε-M: Euler angle coloring; (c) orientation map, α′-M: Euler angle coloring; (d) pole figures of γ with deformation twins; (e) pole figures of ε-M; (f) pole figures of α′-M, one variant. (For interpretation of the references to color in this figure legend, the reader is referred to the web version of the article.)

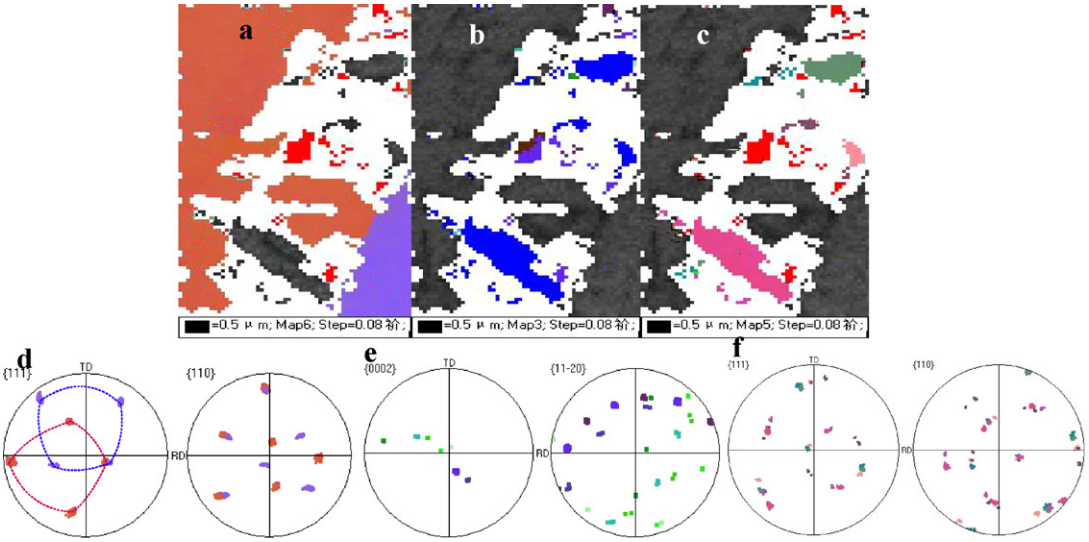

Fig. 9. Martensitic transformation at an annealing twin whose orientation closed to ⟨1 2 4⟩-oriented γ under 10% compression. (a) Orientation map, γ: Euler angle coloring; (b) orientation map, ε-M: Euler angle coloring; (c) orientation map, α′-M: Euler angle coloring; (d) pole figure of γ showing a pair of twins; (e) pole figure of ε-M; (f) pole figure of α′-M showing several variants. (For interpretation of the references to color in this figure legend, the reader is referred to the web version of the article.)

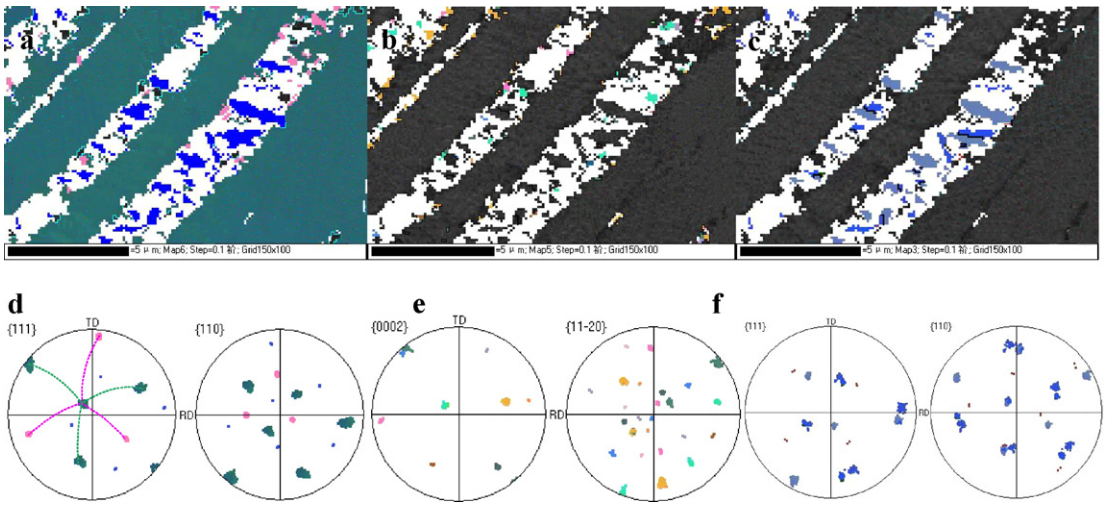

Fig. 10. Martensitic transformation in ⟨1 1 2⟩-oriented γ under compression 10%. (a) Orientation map, γ: Euler angle coloring; α′-M: azure; (b) orientation map, ε-M: Euler angle coloring; (c) orientation map, α′-M: Euler angle coloring; (d) pole figure of γ with twin relationship; (e) pole figure of ε-M; (f) pole figure of α′-M. (For interpretation of the references to color in this figure legend, the reader is referred to the web version of the article.)

⟨1 2 4⟩-oriented γ (orange color in Fig. 9a, d, c, f), which again shows the strong influence of austenitic orientation. In addition, coherent austenitic twin boundaries appear to promote the martensitic transformation in this case. Two ε-M variants were observed at this annealing twin boundary; the large un-indexed area in the orientation map was attributed as soft ε-M phase and the high strain indicates that the ε-M in this austenite grain transformed more slowly than ε-M in ⟨1 0 0⟩-oriented γ. One of the α′-M variants has a stable ⟨1 1 1⟩ orientation (the dark green color in Fig. 9c, f), whereas the other (the pink one in Fig. 9c) is unstable. This example shows the influence of the austenitic orientation and the effect of annealing twin boundaries. The annealing twin boundary promotes nucleation of martensite, but with less variant selection than otherwise expected.

Fig. 10 shows an orientation map in a ⟨1 1 2⟩-oriented γ grain after 10% compression. Only one ε-M band is observed, in which several α′-M variants have formed. Clearly, these variants were produced by the intersection of austenitic twinning (Fig. 10a, d) or other ε-M variants (Fig. 10b, e). In addition, many small ε-M variants were also produced. It can also be noticed that most of the α′-M variants are ⟨1 1 0⟩-oriented α′-M, an unstable orientation during compression. Austenitic mechanical twins are present in the ε-M plates, which provides additional evidence for the influence of twinning on the martensitic transformation. From a comparison of the area fractions of ε-M (mainly the un-indexed region within the bands) and α′-M, it can be found that α′-M is relatively difficult to form in this austenitic orientation.

Fig. 11 shows an orientation map for a unstable ⟨1 1 1⟩-oriented γ grain after 20% compression. Several α′-M variants were formed in this grain, and among them the largest was ⟨1 1 0⟩-oriented α′-M, which should be also less stable during compression. The larger deformation of 20% does not lead to an increase in the number of α′-M variants, but does result in more un-indexed areas of ε-M. This is because due to its softness and easily deformable nature, more ε-M can be produced, consequently more crystal defects appeared, therefore inhibited the formation of α′-M.

Fig. 12 shows an orientation map in a ⟨1 1 0⟩-oriented γ grain after 20% compression. Only one ε-M plate is observed and small ⟨1 1 0⟩/⟨1 0 0⟩ α′-M grains have formed in the thicker ε-M, indicating the difficulty in the formation of α′-M in the thinner ε-M and the influence of the ε-M plate thickness on the formation of α′-M. These observations demonstrate that deformation twins (Fig. 12e) can help to produce stress concentrations, thereby promoting the formation of α′-M in single ε-M. It is noted that ε-M can be easily detected in this case, in contrast with all the previously described grains/regions. This difference may be related to the stability of the initial ⟨1 1 0⟩-oriented γ, as it does not undergo a large orientation change during compression. It is noted further that mechanical twins of ε-M can be detected (the blue region/orientation in Fig. 12b, e). However, most stable ⟨1 1 0⟩ austenitic grains after heavy compression were rotated from initial unstable orientations and thus contained more crystal defects and exhibited a suppressed transformation.

4. Discussion

4.1. Orientation dependency of martensitic transformation and the influence of deformation twinning

The EBSD results clearly show that, similar to twinning in austenite, martensitic transformation depends on the austenitic orientation, more specifically that it proceeds faster in austenite oriented approximately within the ⟨1 0 0⟩–⟨1 1 3⟩–⟨0 1 2⟩ region, which is in accordance with Zhang et al. [6]. Austenite with such orientations favors mechanical twinning or Shockley dislocation movement with prominent variant selection and can reduces the extent of grain refinement due to α′-M formation. Thus different austenitic orientations can lead to differences in the number of variants and the grain sizes of transformed α′-M, and a difference in transformation rates and strain accumulation within the ε-M (discussed later). According to the prediction of Creuziger and Foecle [5], the martensitic transformation rate in differently orientated γ is expected to only vary slightly during compression, except for compression along the ⟨1 1 1⟩-direction, in which martensite transformed most slowly, *and a little bit faster in cube- than in brass-orientations*. Based on our experimental result, the transformation in ⟨1 0 0⟩-oriented γ was clearly easy and only one α′ M developed. Therefore the variant selection was clearly dominant in nearly ⟨1 0 0⟩-oriented austenite. It is further noted that deformation twins were detected in nearly all cases and that the main ε-M variant always formed at twin boundaries, which indicates direct promotion of the transformation by austenitic twinning.

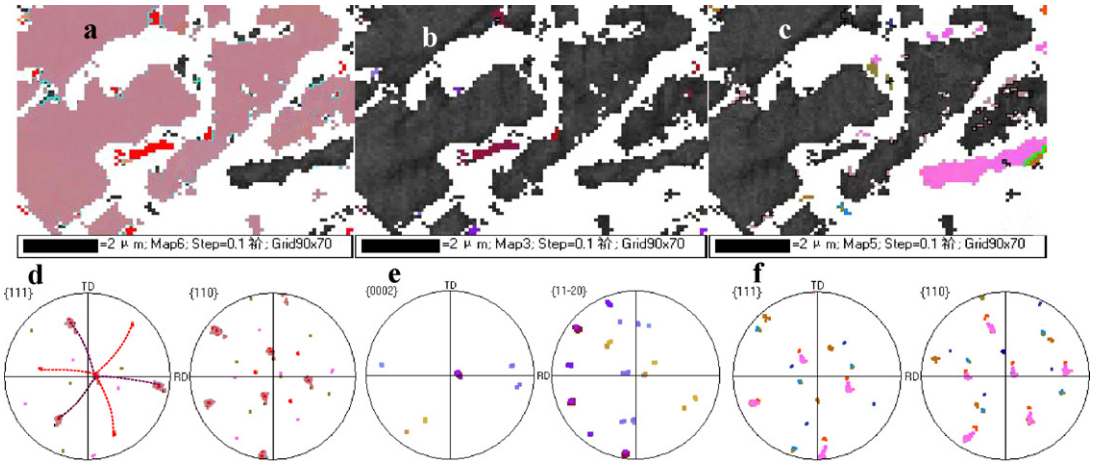

Fig. 11. Martensitic transformation in ⟨1 1 1⟩-oriented γ under 20% compression. (a) Orientation map, γ: Euler angle colorings; (b) orientation map, ε-M: Euler angle coloring; (c) orientation map, α′-M: Euler angle colorings; (d) pole figure of γ showing a pair of twins; (e) pole figure of ε-M; (f) pole figure of α′-M showing several variants. (For interpretation of the references to color in this figure legend, the reader is referred to the web version of the article.)

4.2. Behavior of ε-M during the TRIP process

TRIP steels with a $\gamma \rightarrow \varepsilon \rightarrow \alpha'$ transformation sequence show quite complicated microstructure evolution due to the presence of hexagonal ε-M [4]. The γ-orientation dependency of α′-M is first of all due to the dependency of ε-M on the γ orientation. In the condition of the change of ε-M orientation, slip or twinning may occur within ε-M leading to different interaction between slip and twinning and thus yielding different configurations of crystal defects. This is expected to affect the kinetics of following α′-M transformation, though this is an area that requires further investigation. Due to its softness and unstable orientation during compression, more crystal defects may be expected to appear in ε-M (as evidenced by large un-indexed areas in EBSD orientation maps) and thereby suppress the α′-M transformation,. Furthermore, the intersection of two ε-M plates or one ε-M plate and one twin band is necessary to produce α′-M through high local strain concentration and a combination of two invariant plane strains. A higher area ratio of α′-M to ε-M (including most of the un-indexed regions) was observed in ⟨1 0 0⟩-oriented γ, which demonstrates that ε-M variants in ⟨1 0 0⟩-oriented γ can most easily transform into α′-M. In contrast the large un-indexed area of ε-M in other-oriented γ indicates that high strain can prevent the formation of α′-M. It is not clear whether the high strain of un-indexed regions in ε-M was mainly due to strain transfer from harder and multi-variant α′-M or due to accumulated crystal defects from slip or twinning of ε-M as a results of its unstable orientation during compression.

4.3. The texture effect during TRIP

The texture in α′-M affects both mechanical properties and work hardening behavior of TRIP steels, and thus it is worth of discussion here. If there were no variant selection, there would be no transformation texture developed, as is normally the case for thermally induced martensitic transformation in similar steels. The data presented in this paper show however the dominant transformation that mainly only one variant (of ⟨1 0 0⟩ orientation) is transformed in ⟨1 0 0⟩ austenitic grains during the TRIP process. However, only

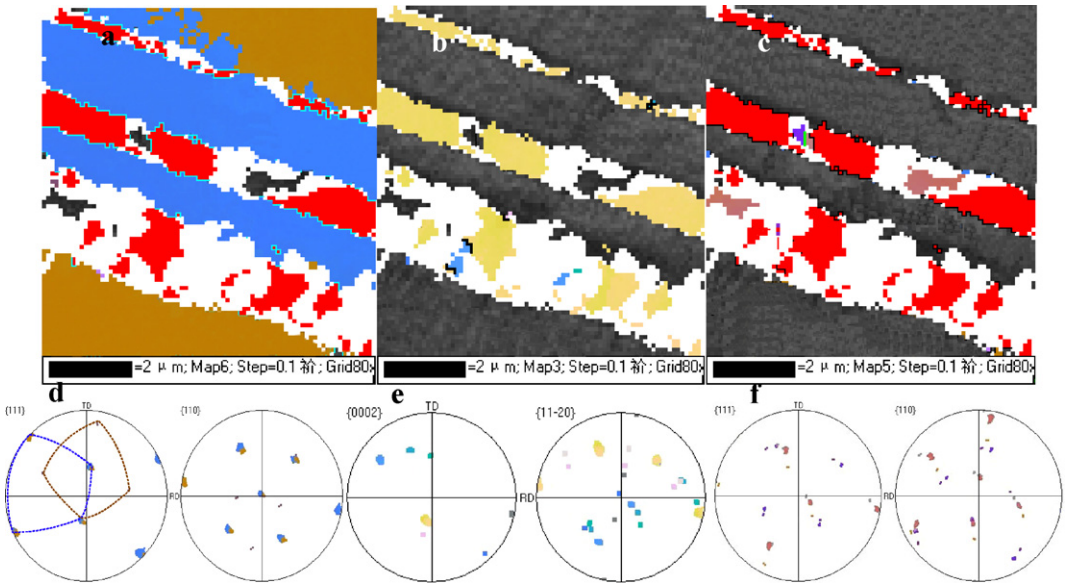

Fig. 12. Orientation imaging of martensitic transformation in {1 1 0} oriented γ under 10% compression. (a) Orientation map, γ: Euler angle coloring; (b) orientation map, ε-M: Euler angle coloring; (c) orientation map, α′-M: Euler angle coloring; (d) pole figure of γ showing a pair of twins; (e) pole figure of ε-M; (f) pole figure of α′-M showing several variants. (For interpretation of the references to color in this figure legend, the reader is referred to the web version of the article.)

less than half of the total austenite has an initial orientation near ⟨1 0 0⟩ orientation. It is necessary therefore to analyze the overall effect of the α′-M transformation on the bulk texture. In addition, since TRIP-H steels show excellent elongation of generally over 50%, the presence of a strong deformation texture after heavy strain can be expected. Therefore, it is necessary also to determine whether the transformation texture, if any, at the early stage of TRIP is affected by the deformation texture developed during later stages of straining. A third question to be answered is that, when both ⟨1 0 0⟩ and ⟨1 1 0⟩ α′-M can be formed in ⟨1 0 0⟩ austenite according to the K–S OR, why is only ⟨1 0 0⟩ α′-M observed during experiments.

Based on the data presented in Section 3, it is seen that at strains of 20–30% the α′-M grains formed in austenite with orientations towards ⟨1 0 0⟩ predominantly have ⟨1 0 0⟩ orientation and have large sizes than α′-M grains formed in austenite of other orientations. Thus a ⟨1 0 0⟩ transformation texture will exist and should contribute to the work hardening behavior. With increasing strain the deformation texture of ⟨1 0 0⟩α will develop and further enhance the transformation texture. Considering the initial α-ferrite in the material investigated in this study it was difficult to separate the final α′-M texture from that of α-ferrite using XRD. However, we have measured the final texture in α′-M after a compression of 50% in a TRIP steel with composition of Fe–0.0045C–17.48Mn–3.04Si–1.80Al, which does not contain ferrite, and this shows a dominant ⟨1 0 0⟩ texture in the α′-M [15]. In other words a ⟨1 0 0⟩ transformation and deformation texture will be present during TRIP process. Finally, we attribute the dominant ⟨1 0 0⟩-, rather than ⟨1 1 0⟩-, oriented α′-M to its more stable orientation with lowest deformation stored energy and low deformation resistance.

5. Conclusions

Based on experimental data on a compressed high manganese TRIP steel obtained by optical microscopy, X-ray diffraction, scanning electron microscopy and EBSD investigations, the following conclusions have been obtained:

(1) The austenite to α′-M transformation took place more easily in ⟨1 0 0⟩-oriented γ, and was such that only one variant of ⟨1 0 0⟩-oriented α′-M was produced. Consequently the transformation to α′-M failed to produce grain refinement, in contrast to the case for thermally induced martensitic transformation where no variant selection takes place. This effect of deformation on the non-diffusive transformation differs to that of strain-induced diffusive transformations, where grain refinement always takes place due to enhanced nucleation with increasing strain. In γ-grains of other orientations several α′-M variants can be formed but in each case fewer variants are seen than in similarly oriented grains for the case of thermally induced martensite.

(2) Similar to twinning in austenite, the formation of ε-M is also affected by the austenitic orientation. It was found that ε-M occurring in ⟨1 0 0⟩-oriented γ can transform more smoothly into α′-M than ε-M in austenite grains of other orientations. The deformation due to plastic strains is differently distributed in the γ, α′-M and ε-M phases. Higher strains are mainly distributed in the softer ε-M, resulting in more un-indexed regions in the ε-M during EBSD measurement. Thicker ε-M can quickly induce α′-M due to a smaller strain accumulation caused by the harder α′-M during transformation. The EBSD measurements also show that more ε-M variants develop, and these are of smaller size during TRIP deformation than seen in thermally induced martensite.

(3) Due to a preferred transformation in ⟨1 0 0⟩-oriented γ and the preferred ⟨1 0 0⟩$_\alpha$ stable orientation of α′-M where only one variant is developed, a ⟨1 0 0⟩ texture is formed easily in compressed TRIP steels. However, the larger number of variants formed in other oriented austenitic grains and the effect of annealing twin boundaries as preferred nucleation sites for martensite both act to weaken formation of the transformation texture. In addition, the stable ⟨1 1 0⟩ texture of austenite hinders transformation and produces a mechanical stabilization.

Acknowledgements

This study was financially supported by the Chinese National Natural Science Foundation (No.: 50771019) and the Specialized Research Fund for the Doctoral Program of Higher Education (No.: 20090006110013).

References

[1] C.L. Magee, Ph.D. Thesis, Carnegie Institute of Technology, Pittsburgh, PA, 1966.
[2] G.W. Greenwood, R.H. Johnson, Proc. R. Soc. Lond. A 283 (1965) 403–422.
[3] I.V. Kireeva, Y.I. Chumlyakov, Mater. Sci. Eng. A 481–482 (2008) 737–741.
[4] B. Petit, N. Gey, M. Cherkaoui, B. Bolle, M. Humbert, Int. J. Plast. 23 (2007) 323–341.
[5] A. Creuziger, T. Foecle, Acta Mater. 58 (2010) 85–91.
[6] M.X. Zhang, P.M. Kelly, J.D. Gates, Mater. Sci. Eng. A 273–275 (1999) 251–256.
[7] E. Nagy, V. Mertinger, F. Tranta, J. Sólyom, Mater. Sci. Eng. A 378 (2004) 308–313.
[8] O. Grässel, L. Krüger, G. Frommeyer, L.W. Meyer, Int. J. Plast. 16 (2000) 1391–1409.
[9] M. Karlsen, Ø. Grong, M. Sfferud, J. Hjelen, G. Rrvik, R. Chiron, Metall. Mater. Trans. A 40 (2009) 310–320.
[10] L. Bracke, L. Kestens, J. Penning, Scripta Mater. 57 (2007) 385–388.
[11] S.H. Hong, Y.S. Han, Scripta Metall. Mater. 32 (1995) 1489–1494.
[12] T. Kirindi, M. Dikici, J. Alloys Compd. 407 (2006) 157–162.
[13] S. Zaefferer, J. Ohlert, W. Bleck, Acta Mater. 52 (2004) 2765–2778.
[14] L Meng, P. Yang, Q. Xie, H. Ding, Z. Tang, Scripta Mater. 56 (2007) 931–934.
[15] P. Yang, F.-Y. Lu, L. Meng, F.-E. Cui, Acta Metall. Sin. 46 (2010) 666–673 (in Chinese).